

# LABORATORY BOREHOLE MODEL

by

E. R. Shortt

Earth Resources Laboratory  
Department of Earth, Atmospheric, and Planetary Sciences  
Massachusetts Institute of Technology  
Cambridge, MA 02139

## ABSTRACT

An experimental method for acquisition of full waveform acoustic logging (FWAL) data from scaled laboratory borehole/formation models is under development. A spark-gap source, fabricated in the lab, is used in conjunction with a piezoelectric receiver. It is found that the source/receiver signature covers a suitable frequency range for the 32:1 scaling required by the 6.4 mm model borehole diameter. Waveforms collected from water-filled boreholes in aluminum and Lucite, simulating fast and slow formations, clearly exhibit the characteristic arrivals of those formations.

## INTRODUCTION

Laboratory acquisition of FWAL data from scaled borehole/formation models will provide an opportunity to test existing and developing techniques of log analysis. Data collected in a controlled environment, i.e., from simple models described by a few easily measured parameters, are well suited for comparison with the results of theoretical modeling. This approach will aid in understanding the discrepancy between synthetic and observed data due to assumptions and approximations within the theory and uncertainties of the actual well. The few published accounts of studies in this area are listed here as references.

## EXPERIMENTAL METHOD

The effort to date in the Ultrasonics Modeling Lab at ERL has been toward fabrication of a suitable source and development of a basic experimental method. A block diagram of the experimental setup is shown in Figure 1. A spark-gap source and piezoelectric receiver are positioned in the water-filled borehole of the model formation. The high voltage pulse generator supplies energy to produce a spark at the source tip. This impulsive acoustic source excites various waves in the elastic medium which are detected

by the acoustic disturbances they create at the receiver. The resulting electronic signal is fed to the ultrasonic analyzer for amplification and, if selected, filtering and gating. The amplified signal is then digitally stored and displayed by the transient capture oscilloscope. The analyzer and scope are triggered by a timing pulse from the pulse generator. The records are stored on floppy disc and later transferred via an IBM PC/AT to the Vax 11/780. The data are then formatted for further processing and convenient use by the FWAL group at the laboratory.

### Source and Receiver

The model receiver in these initial experiments is a commercially available hydrophone. The package consists of a 2 mm diameter thin-walled cylindrical lead zirconium titanate (PZT) crystal embedded in a damping medium. The unit is mounted at the end of a stainless steel tube through which a BNC connection is made. The active element is protected by a rubber sleeve. The excitation of a source/receiver pair of hydrophones arranged side by side in open water shows a resonance peak at 1.0 MHz.

The source currently in use is essentially the same spark-gap type as described by Roever and Vining (1959). A pair of electrodes separated by a small gap are subjected to a high differential voltage, producing a spark. A square pulse of 1  $\mu$ s duration will jump a 0.025 mm gap at 0.5 kV in air and 1.0 kV in water. The effect of using distilled and deionized water versus tap water is negligible.

The spark source is fabricated using a 20 cm long 20 gauge (0.9 mm o.d.) stainless steel hypodermic needle as the ground electrode. The spark gap is between the faced needle tip and the exposed end of 28 gauge (0.25 mm wire o.d., 0.48 mm insulation o.d.) Kynar insulated single strand wire which is fed through the needle. The gap is adjusted by positioning the wire with the aid of a jeweler's loop and locking it in place with a set screw. The adjustment is considered satisfactory when the minimum voltage at which a pulse of 1  $\mu$ s duration consistently produces a spark in water is between 1.0 and 1.2 kV.

The observed variability in the brightness and sound of the spark from shot to shot is seen in the acoustic signal detected by the hydrophone. Apart from the perhaps 1 shot in 10 or 15 which is clearly a "miss", the amplitude of the signal varies by approximately a factor 2. Averaging over 10 waveforms appears to provide consistency and will be employed later in the experiments. Sample source/receiver signatures recorded in open water are shown in Figure 2. The spectral content of the pair covers frequencies below 0.6 MHz with an additional peak due to receiver response centered at 1.0 MHz.

The spark source deteriorates after approximately 400 shots. The wire tip is then clipped, a fresh section stripped, the needle tip faced with a file, and the gap adjusted.

## Model Formation/Borehole

Experimental objectives require that the scaling of the model formation/borehole keeps the ratio of wavelength to borehole radius constant. The most convenient arrangement is to choose model materials to match bulk properties of the formation of interest and to adjust the frequency content of the source according to the linear dimensions of the model. A model borehole diameter of 6.4 mm is used in this first set of experiments, requiring a scaling factor of 32 for a 20 cm diameter borehole. Applying this to the typical frequencies used in the field, 5 to 20 kHz, the spectrum of the spark source and receiver pair is seen to cover a suitable range, 100 to 600 kHz. Note that since the receiver response is centered at 1 MHz, frequencies higher than those of primary interest will be selectively amplified.

Aluminum and Lucite are used as preliminary approximations of hard ( $v_s > v_f$ ) and soft ( $v_s < v_f$ ) formations (Table 1). The size of the pieces (20 cm diameter  $\times$  30 cm long) was chosen to avoid the complication of boundary reflections for source/receiver separations up to 6.5 cm, corresponding to a scaled separation of more than 2 m. The holes were drilled and reamed, producing a very good surface finish. The source and receiver are held in position with tightly fitting spacers that are located toward the boundaries of the model. Accumulated bubbles produced by electrolysis must be flushed from the horizontal borehole. Later experiments will be performed with the model in an upright position.

## EXPERIMENTAL RESULTS

Preliminary data consist of records collected from the aluminum and Lucite models for varying source/receiver separation. Included are examples illustrating the effect of an offcenter source in Lucite. The signals were not filtered except for the fixed lowpass 5 MHz input filter on the oscilloscope. The digitization interval of the 4096 data points per record is 27.7 ns.

### Discussion

Waveforms collected from the aluminum model with the source/receiver separation incremented by 1 cm are shown in Figure 3. The distinct arrivals are identified as the two refracted body waves, compression (P) and shear (S), and the direct fluid (F) wave. The velocities corresponding to the moveout curves are:  $v_p = 6.3$  km/s,  $v_s = 3.1$  km/s, and  $v_f = 1.5$  km/s. These values agree well with those of Table 1. The large amplitude of the fluid arrival is due to both the large amplitude of the direct acoustic wave and the center frequency of the receiver. In Figure 4, increased amplification of the signal before acquisition more clearly shows the energy arriving in the time interval between

the P and S arrivals. This is attributed to the leaky mode of the P wave.

Waveforms produced from the same experiment performed with the Lucite model are shown in Figure 5. Three arrivals are clearly visible and are identified as the P wave, the direct fluid wave, and the Stoneley (ST) wave. The velocities corresponding to the moveout curves are:  $v_p = 2.6$  km/s,  $v_f = 1.5$  km/s, and  $v_{st} = 1.1$  km/s. The low frequency and a velocity near  $0.9 v_f$  are typical characteristics of the Stoneley wave.

Examples of waveforms illustrating the effect of varying the source position with respect to the borehole axis in Lucite are shown in Figure 6. The amplitude and period of the Stoneley wave are significantly increased for the case of an offcenter source. Note that the period of the Stoneley wave for the centered case is less than that seen in Figure 5. This indicates the need for greater attention to source/receiver positioning.

## CONCLUSIONS

Preliminary experiments performed on simple models using the spark source and PZT receiver show that the basic experimental method is satisfactory. The waveforms exhibit arrivals characteristic of FWAL data. Improvements will be made before proceeding to more complicated models and comparison with synthetics. The source/receiver positioning procedure must be modified and the effects of position investigated further. Data quality improvement through averaging during acquisition will be employed. It is also anticipated that appropriate filtering of waveforms will enhance the phase arrivals.

## ACKNOWLEDGEMENTS

This research is supported by the Full Waveform Acoustic Logging Consortium at M.I.T.

## REFERENCES

- Chen, S. T., 1982, The full acoustic wave train in a laboratory model of a borehole; *Geophysics*, 47, 1512-1520.
- Roever, W. L., and Vining, T. F., 1959, Propagation of elastic wave motion from an impulsive source along a fluid/solid interface: I. Experimental pressure response; *Phil. Trans. R. Soc. Lon.*, A251, 455-465.
- Roever, W. L., Rosenbaum, J. H., and Vining, T. F., 1974, Acoustic waves from an impulsive source in a fluid-filled borehole; *J. Acoust. Soc. Am.*, 55, 1144-1157.

Rosenbaum, J. H., 1974, Synthetic microseismograms: logging in porous formations; Geophysics, 39, 14-32.

Schoenberg, M., Marzetta, T., Aron, J., and Porter, R. P., 1981, Space-time dependence of acoustic waves in a borehole; J. Acoust. Soc. Amer., 70, 1496-1507.

Table 1: Properties of model materials and idealized formations. Compressional and shear velocities,  $v_p$  and  $v_s$ , density  $\rho$ , and Poisson ratio,  $\nu$ .

	$v_p$ (km/s)	$v_s$ (km/s)	$\rho$ (g/cc)	$\nu$
6061 aluminum	6.5	3.1	2.7	.35
cast Lucite	2.6	1.2	1.2	.36
fast formation	4.9	2.6	2.1	.30
slow formation	3.0	1.3	2.0	.38
water	1.5	-	1.0	-

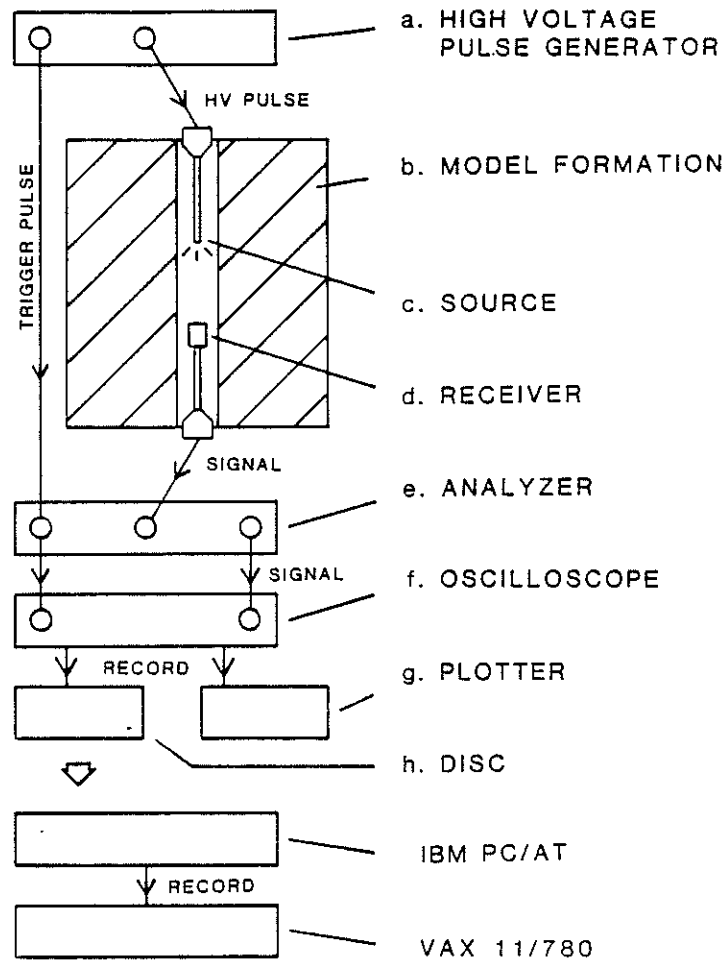


Figure 1: Block diagram of experimental setup. a) Velonex 350 pulse generator. b) Model formation with water-filled 6.4 mm borehole. c) Spark-gap source. d) Celesco LC-5 hydrophone. e) Panametrics ultrasonic analyzer - amplifier, filter, and gate. f) Data Precision 6000 oscilloscope with 630 plug-in. g) HP 7470A plotter. h) Data Precision dual disc unit.

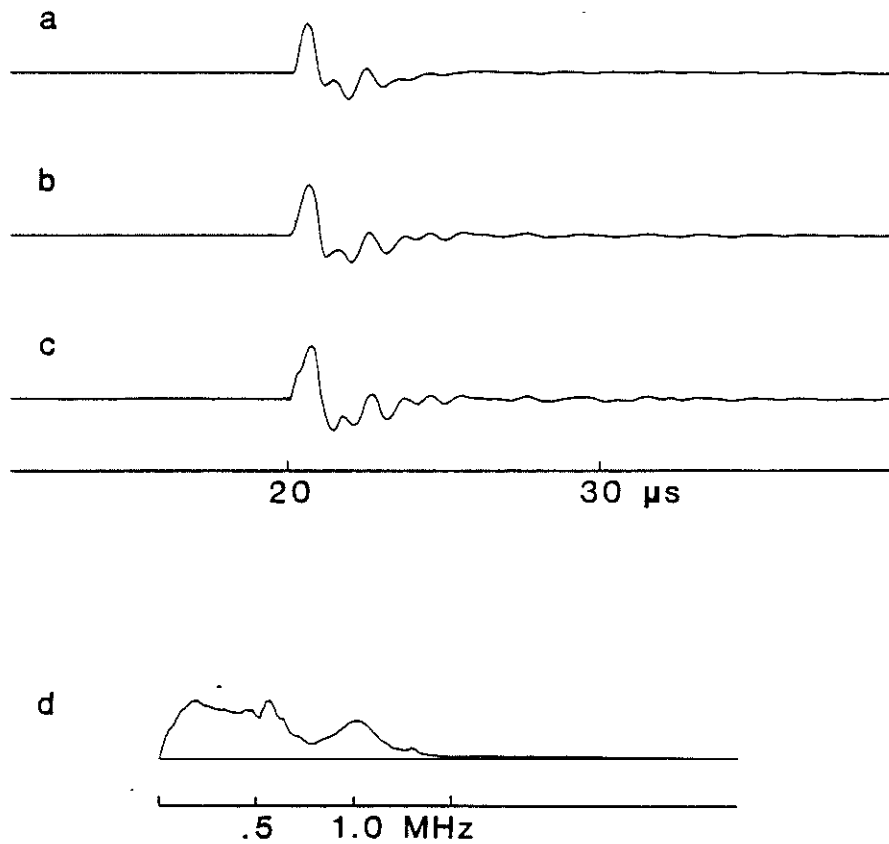


Figure 2: Signature from spark source and piezoelectric receiver in open water before and after experiment with aluminum model. Voltage pulse to source is 1.2 kV, 1.7  $\mu\text{s}$  duration. a) Source with fresh tip before experiment, 10 shot average. b) After experiment, 10 shot average. c) After experiment, single shot. d) Spectrum of waveform b.



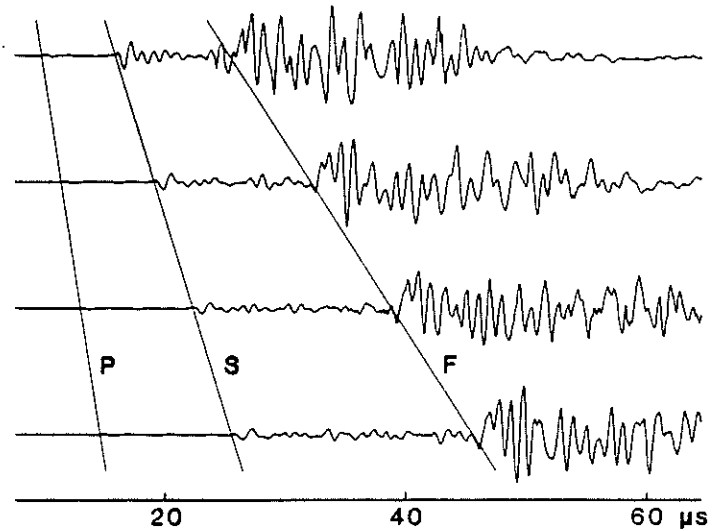


Figure 3: Waveforms recorded in water-filled 6.4 mm diameter borehole in aluminum ( $v_s > v_f$ ). Source/receiver separation is incremented by 1 cm. Moveout is illustrated for three arrivals: compression (P), shear (S), and fluid (F). The corresponding velocities are:  $v_p = 6.3$  km/s,  $v_s = 3.1$  km/s, and  $v_f = 1.5$  km/s.

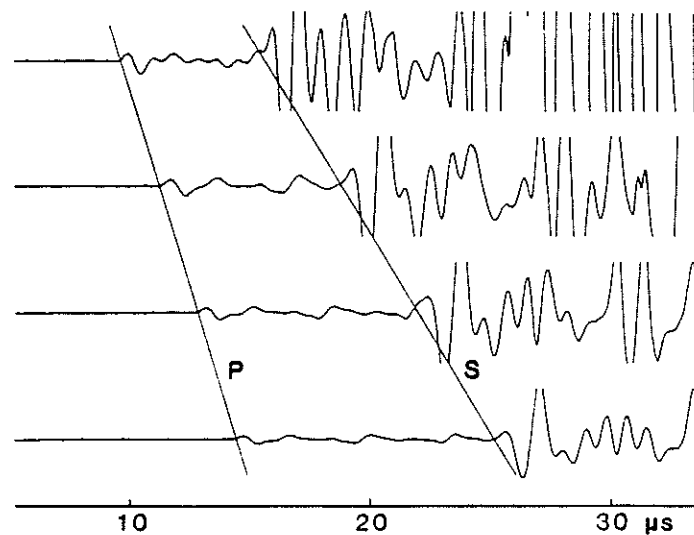


Figure 4: Waveforms recorded in water-filled 6.4 mm diameter borehole in aluminum ( $v_s > v_f$ ). Same configuration as Figure 3 with increased signal amplification before acquisition for better resolution in the interval between the P and S wave arrivals.

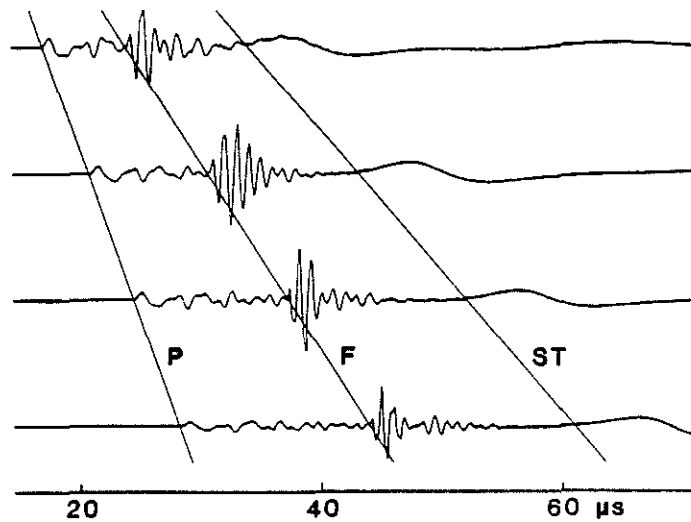


Figure 5: Waveforms recorded in water-filled 6.4 mm diameter borehole in Lucite ( $v_s < v_f$ ). Source/receiver separation is incremented by 1 cm. Moveout is illustrated for three arrivals: compression (P), fluid (F), and Stoneley (ST). The corresponding velocities are:  $v_p = 2.6$  km/s,  $v_f = 1.5$  km/s, and  $v_{st} = 1.1$  km/s.

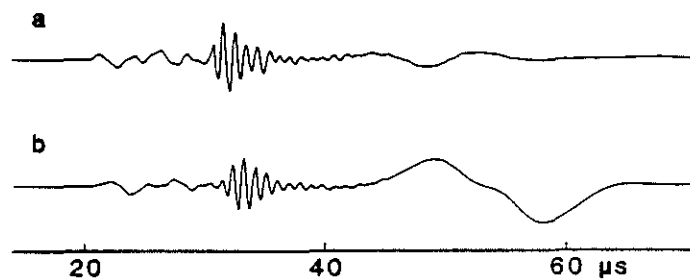


Figure 6: Waveforms recorded in water-filled 6.4 mm diameter borehole in Lucite ( $v_s < v_f$ ). a) Source on borehole axis. b) Source positioned halfway between borehole axis and borehole wall.